


Quantum Mechanical Studies of Three Aromatic Halogen-Substituted Bioactive Sulfonamidobenzoxazole Compounds with Potential Light Harvesting Properties

Y. Sheena Mary, Tugba Ertan-Bolelli, Renjith Thomas, Akhil R. Krishnan, Kayhan Bolelli, Esin Nagihan Kasap, Tijen Onkol & Ilkay Yildiz


To cite this article: Y. Sheena Mary, Tugba Ertan-Bolelli, Renjith Thomas, Akhil R. Krishnan, Kayhan Bolelli, Esin Nagihan Kasap, Tijen Onkol & Ilkay Yildiz (2021) Quantum Mechanical Studies of Three Aromatic Halogen-Substituted Bioactive Sulfonamidobenzoxazole Compounds with Potential Light Harvesting Properties, *Polycyclic Aromatic Compounds*, 41:7, 1563-1579, DOI: [10.1080/10406638.2019.1689405](https://doi.org/10.1080/10406638.2019.1689405)

To link to this article: <https://doi.org/10.1080/10406638.2019.1689405>

 View supplementary material 

 Published online: 11 Nov 2019.

 Submit your article to this journal 

 Article views: 238


 View related articles 

 View Crossmark data 

 Citing articles: 18 View citing articles 



Quantum Mechanical Studies of Three Aromatic Halogen-Substituted Bioactive Sulfonamidobenzoxazole Compounds with Potential Light Harvesting Properties

Y. Sheena Mary^a, Tugba Ertan-Bolelli^b, Renjith Thomas^c , Akhil R. Krishnan^d, Kayhan Bolelli^b, Esin Nagihan Kasap^e, Tijen Onkol^f, and Ilkay Yildiz^b

^aDepartment of Physics, Fatima Mata National College (Autonomous), Kollam, Kerala, India; ^bFaculty of Pharmacy, Department of Pharmaceutical Chemistry, Ankara University, Yenimahalle, Ankara, Turkey; ^cDepartment of Chemistry, St. Berchmans College (Autonomous), Changanassery, Kerala, India; ^dDepartment of Physics, Malabar Christian College, Kozhikode, Kerala, India; ^eFaculty of Pharmacy, Department of Basic Sciences, Gazi University, Ankara, Turkey; ^fFaculty of Pharmacy, Department of Pharmaceutical Chemistry, Gazi University, Ankara, Turkey

ABSTRACT

Three different organic compounds, 2-phenyl-5-(4-trifloromethyl phenyl sulfonamido) benzoxazole (PTPS), 2-(4-chlorobenzyl)-5-(2,4-dinitrophenylsulfonamido)benzoxazole (CNSB) and 2-(4-fluorobenzyl)-5-(2,4-dinitrophenylsulfonamido)benzoxazole (FBPS), were synthesized. To find their energetically stable conformation, geometry optimization was done using density functional theory with the level B3LYP/cc-pVDZ. Electron distribution of the system was studied using molecular electrostatic potential map. Different intermolecular interactions arising from hyperconjugative effect were investigated using the natural bond orbital (NBO) formalism. Nonlinear optical properties were further studied using first-order hyperpolarizability values. The three compounds may be important in the development of novel inhibitor molecules of Topoisomerase II enzyme, as lead compounds. Light harvesting efficiency of PTPS is 0.9342, which shows that it is having potential applications in the design of new DSSC's.

ARTICLE HISTORY





Received 11 June 2019
Accepted 1 November 2019

KEYWORDS


Benzoxazole; DFT; DSSC; LHE; molecular docking

Introduction

Benzoxazole ring system exhibits various biological activities such as antimicrobial and antitumor.^{1–4} 2-(4-Chlorobenzyl)-5-(2,4-dinitrophenylsulfonamido) benzoxazole (CNSB) and 2-(4-fluorobenzyl)-5-(2,4-dinitrophenylsulfonamido) benzoxazole (FBPS) were prepared for their antimicrobial activity.⁵ They showed moderate effect against Gram-positive bacteria *Staphylococcus aureus* and its clinical isolate with 16 µg/mL minimum inhibition concentration. In 2018, compound 2-phenyl-5-(4-trifloromethyl phenyl sulfonamido) benzoxazole (PTPS) was synthesized and evaluated for inhibitory activities *in vitro* against hGST P1-1 enzyme and found to be more effective than the standard compound Etachrinic acid.³ The deoxyribonucleic acid (DNA) topoisomerases (Topo) enzyme is an essential biocatalyst that is very important in the solution of various topological issues related to DNA transcription, recombination, chromatin assembly, repair, and replication, in the regulation of

CONTACT Renjith Thomas  renjith@sbcollege.ac.in  Department of Chemistry, St. Berchmans College (Autonomous), Changanassery, Kerala, 686101, India; Ilkay Yildiz  iyildiz@pharmacy.ankara.edu.tr  Faculty of Pharmacy, Department of Pharmaceutical Chemistry, Ankara University, Yenimahalle, Ankara, 06560, Turkey.

Color versions of one or more of the figures in the article can be found online at www.tandfonline.com/gpol.

 Supplemental data for this article is available online at <https://doi.org/10.1080/10406638.2019.1689405>.

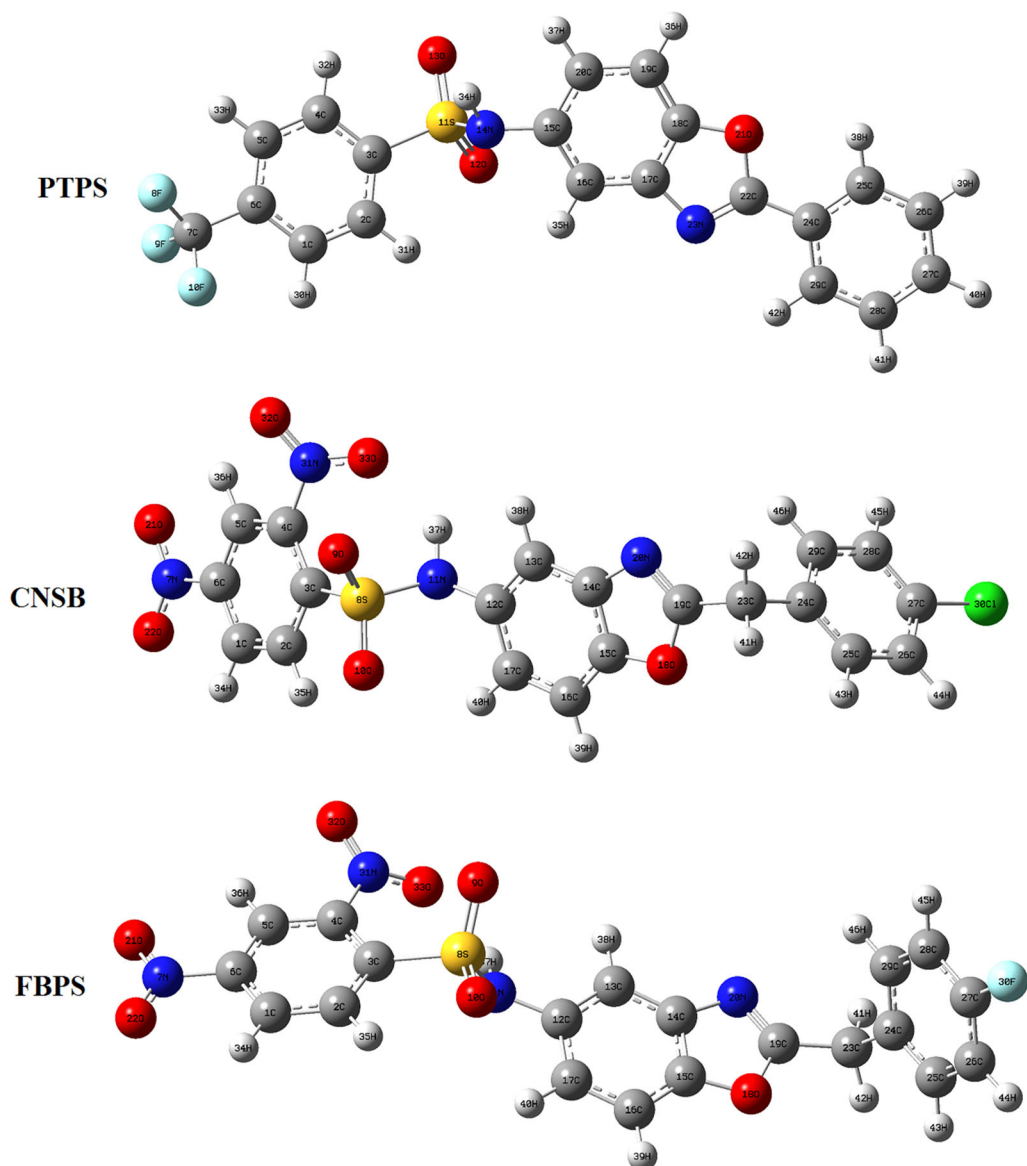


Figure 1. Optimized structures of the compounds PTPS, CNSB, and FBPS using B3LYP/cc-pVDZ.

DNA topology.⁶ Vibrational spectroscopic studies of a number of benzoxazole and sulfonamido derivatives are reported by Mary et al.^{7–11} In this study, three reported benzoxazole compounds (Figure 1) are subjected to various spectral investigations.⁵ Later it was subjected to computational studies. Density functional theory is used to study various factors that govern physical and chemical characteristics of a compound.^{12,13} This paper reveals the quantum chemical studies of particular compounds to give relation between experimental and theoretical results. Also, in this study, PTPS, CNSB, and FBPS were subjected to active site molecular docking studies of human topoisomerase II enzyme in order to predict their protein–ligand interaction. This manuscripts aims to establish the geometry of the molecules under study, and compare and predict the experimental and simulated spectra and other quantum mechanical descriptors to give information about various physicochemical phenomena.

Experimental and computational details

The preparation of the title compounds are as in the literature.^{2,4,14–16} Raman spectra is determined using Delta Nu Raman microscope with a 785 nanometer laser and a CCD detector from DeltaNu Inc (Laramie, WY). 150-mW laser power for 60-s acquisition time was employed, followed by a base line correction for all measurements in the range 200–2000 cm^{-1} . Gaussview¹⁷ is used for drawing input structures and visualize the outputs if the molecules PTPS, CNSB and FBPS and Gaussian09¹⁸ were used for performing quantum mechanical calculations. In this series, DFT (B3LYP) calculation with the basis set CC-pVDZ was used. The geometrical parameters, NBO and energy distributions (HOMO and LUMO), MESP were analyzed and plotted using Gauss View program.

Results and discussion

The molecular structures of PTPS, CNSB and FBPS are optimized, and the structure is shown in Figure 1. The atoms are labeled and numbered. The total energy of title molecules (PTPS, CNSB, and FBPS) calculated by B3LYP/CC-pVDZ is -1802.8143 , -2373.6647 and -2013.3020 a.u. The infrared vibrational spectrum of the title molecules in the same level of theory shows no imaginary frequencies indicated that the geometry presents a global minimum. Scaling factor of 0.9613 is used to scale the frequencies.¹⁹ This scaled spectral data is compared with experimental IR spectrum as shown in given in Figure 2. Same level of theory was used to simulate the Raman spectrum which is given in Figure 3, and the data shows the comparative frequency values with experimental Raman spectrum and both simulated spectra are found to be in close agreement with experimental spectra.

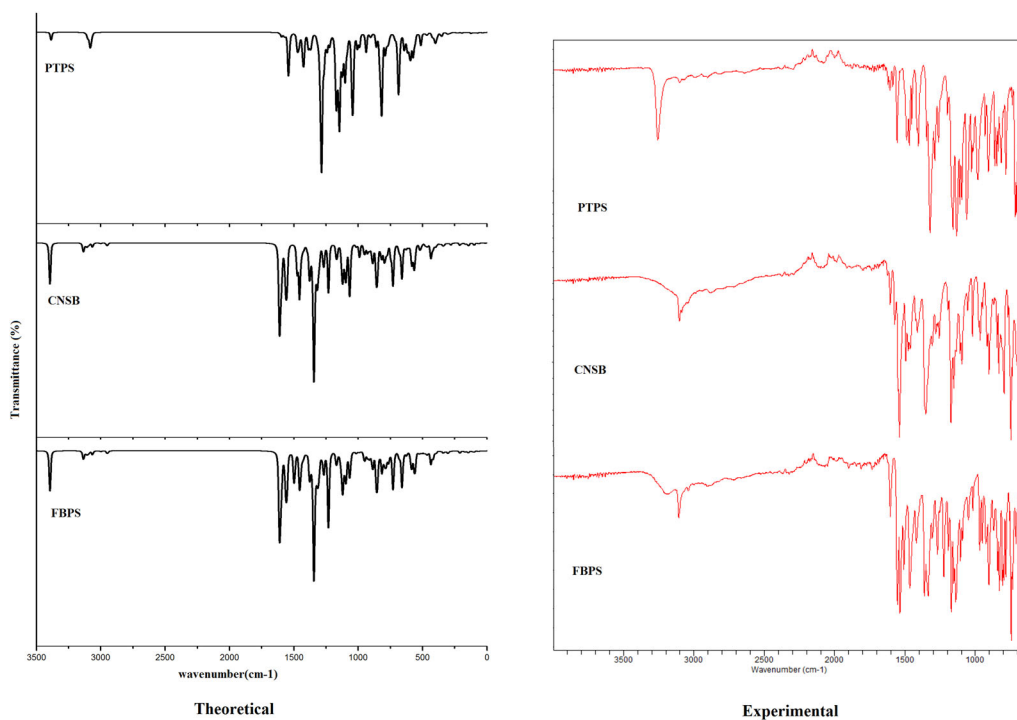


Figure 2. Comparison of experimental and simulated (scaled) IR spectrum of PTPS, CNSB, and FBPS using B3LYP/cc-pVDZ.

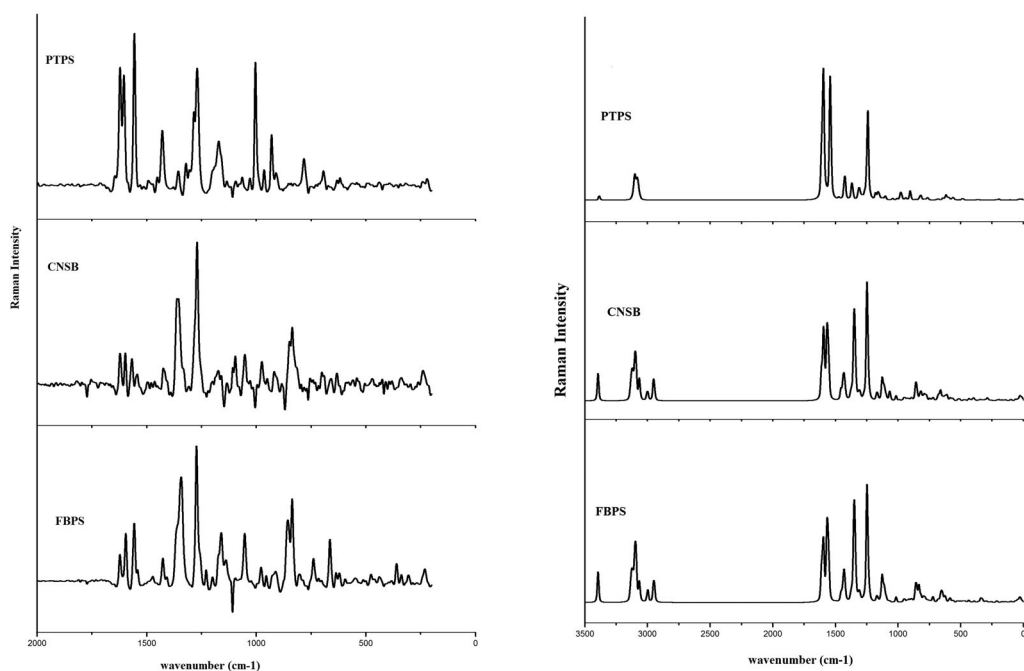


Figure 3. Comparison of experimental and simulated (scaled) Raman spectrum of PTPS, CNSB, and FBPS using B3LYP/cc-pVDZ.

Vibrational assignments

Table 1 presents the vibration assignment of the title compounds. The ν_{CN} (stretch) is observed in the IR region of $1600\text{--}1150\text{ cm}^{-1}$ for benzenoid compounds. The C=N modes are seen at 1550 (PTPS), 1552 (CNSB) and 1560 (FBPS) cm^{-1} experimentally.²⁰ The C-O stretching modes are assigned at around 1271 and 915 cm^{-1} experimentally for all the molecules.²⁰ The SO_2 modes are also around 1265 and 1097 cm^{-1} for all molecules. All the experimentally observed modes are identified and assigned, and they are in close agreement with simulated spectra.

Molecular docking procedure

Docking studies of the compounds PTPS, CNSB, and FBPS were performed by using Schrödinger software.^{21–23} These ligands were prepared by using LigPrep module, and the 2D structures of the ligands were converted to the full 3D structure by assigning the OPLS-2005 force field. LigPrep can generate the expected ionized forms at significant concentrations corresponding to the $\text{pH } 7.0 \pm 3.0$; generate variations and verification; and optimize the structures. It generates maximum 32 stereochemical structures per ligand. Topoisomerase II α is essential for the survival of actively growing cells. Enzyme concentrations are upregulated dramatically during periods of cell proliferation. Furthermore, topoisomerase II α levels increase over the cell cycle and peak in G2/M.²⁴ Topoisomerase II α is found at replication forks and remains tightly associated with chromosomes during mitosis. Thus, topoisomerase II α is believed to be the isoform that functions in growth-dependent processes, such as DNA replication and chromosome segregation. In contrast, expression of the β isoform is independent of proliferative status and the enzyme dissociates from chromosomes during mitosis. Topoisomerase II β cannot compensate for the loss of topoisomerase II α in mammalian cells, and its physiological functions have yet to be defined. Although topoisomerase II β appears to be dispensable at the cellular level, it is required for proper neural development in mice. While the topoisomerase I and topoisomerase II β enzymes

Table 1. FT-IR and FT Raman experimental and scaled theoretical spectra of title compounds with vibrational assignments.

B3LYP/CC-pVDZ $\nu(\text{cm}^{-1})$	IR IRI	RA	$\nu(\text{cm}^{-1})$	Raman $\nu(\text{cm}^{-1})$	Assignments –
PTPS					
3386	16.68	78.64	3256	–	νNH
3083	28.22	269.73	3084	–	νCHIII
3062	0.23	45.60	3045	–	νCHIII
1611	1.46	495.18	–	1618	νPhII
1598	2.31	1821.5	–	1600	νPhIII
1597	7.26	10.30	1596	–	νPhI
1574	12.07	87.72	1573	–	νPhIII
1541	122.84	1897.6	1550	1550	$\nu\text{C} = \text{N}$
1478	1.46	0.60	1480	–	νPhI
1473	30.55	21.81	–	1474	νPhIII
1462	44.54	7.88	1460	1460	δNH
1426	109.84	427.65	–	1426	νPhII
1385	46.66	8.30	1388	1381	νPhI
1368	44.45	278.30	–	1358	νPhII
1316	11.73	92.81	1319	1318	νPhI
1308	5.74	93.88	–	1307	νPhI
1298	25.68	34.60	1298	–	δCHIII
1287	41.92	31.41	–	1286	νCF
1272	4.57	10.03	–	1271	νCO
1265	68.95	52.05	1259	–	νSO_2
1221	31.43	34.62	1225	–	δCHII
1181	16.62	65.69	–	1178	δCHII
1163	17.62	5.21	1162	–	δCHI
1124	127.12	30.12	1128	1126	δCHII
1088	39.76	1.70	1090	1090	δCHI
1070	2.04	1.27	–	1068	δCHII
1043	145.09	16.45	1044	–	νCF
1037	29.67	1.69	1028	1032	δCHIII
1008	29.05	13.61	1016	1005	νPhIII
969	0.09	1.61	–	967	γCHIII
951	0.04	0.27	953	–	γCHI
940	35.68	17.86	–	938	γCHI
904	7.08	90.06	906	906	νCO
860	26.68	5.65	862	–	γCHII
834	33.37	1.72	–	840	γCHI
821	138.42	55.78	–	824	νSN
816	90.78	13.10	816	–	γCHI
791	37.23	8.26	–	788	γCHII
762	19.30	2.86	–	758	γCHIII
722	2.55	0.71	719	–	τPhII
712	9.32	0.88	707	–	τPhI
692	53.72	5.01	–	693	τPhIII
676	13.33	1.51	–	675	τPhIII
641	47.39	23.70	652	539	δPhII
620	20.02	28.05	625	621	δPhI
562	34.22	37.68	–	563	τPhI
554	0.31	1.41	–	550	δCF_3
484	1.27	1.69	–	490	τPhII
467	8.71	0.28	–	468	τPhI
424	13.23	0.95	–	430	τPhII
389	12.03	0.87	–	390	δPhI
360	3.08	2.8	–	361	τCF_3
352	7.68	1.97	–	350	τPhII
277	1.23	1.29	–	280	δPhI
237	0.90	1.01	–	240	τSO_2
226	1.46	2.23	=	225	τCF_3

CF3 phenyl =====I

Middle =====II

Mono=====III

(continued)

Table 1. Continued.

B3LYP/CC-pVDZ $\nu(\text{cm}^{-1})$	IR IRI	RA	$\nu(\text{cm}^{-1})$	Raman $\nu(\text{cm}^{-1})$	Assignments –
CNSB					
3109	8.50	29.81	3109	–	νCHI
3096	4.15	52.26	3094	–	νCHIII
3064	8.58	69.00	3062	–	νCHIII
2951	10.81	16.25	2955	–	νCH_2
1613	188.45	17.28	1615	1617	νNO_2
1596	22.24	194.54	1598	1598	νPhII
1570	34.98	17.70	1573	–	νNO_2
1567	6.62	6.09	1569	1567	νPhIII
1556	93.27	25.95	–	1552	$\nu\text{C}=\text{N}$
1475	69.75	0.20	1480	1482	νPhIII
1455	166.09	41.20	1456	1460	νPhII
1435	17.75	136.0	1432	–	δNH
1421	9.25	29.54	–	1422	δCH_2
1395	12.08	0.74	1394	1393	νPhIII
1351	60.55	282.2	–	1354	νNO_2
1343	382.51	14.50	1343	–	νNO_2
1306	85.92	36.23	–	1306	νPhI
1279	0.51	1.25	1282	–	νPhIII
1270	70.50	5.59	–	1271	νCO
1258	2.61	3.11	1257	–	νSO_2
1232	120.43	9.12	1230	–	δCHII
1223	5.85	2.71	–	1219	δCHI
1170	9.07	9.62	1177	–	δCHIII
1168	41.98	19.66	–	1169	δCHII
1162	8.79	6.34	1163	1159	δCHIII
1129	29.28	4.26	1138	1131	δCHII
1109	10.02	36.8	–	1108	δCHI
1097	86.02	6.80	1097	–	νSO_2
1091	3.86	2.83	–	1093	δCHIII
1066	143.26	19.13	1066	1055	δCHI
1017	7.52	14.96	1025	1027	νPhI
991	36.70	2.58	1000	993	νPhIII
972	0.02	0.76	–	974	γCHI
951	43.89	15.19	953	953	δCH_2
924	2.90	5.94	–	922	γCHIII
911	0.94	0.93	909	–	νCO
887	41.19	2.07	889	886	γCHI
861	77.00	3.73	861	–	γNH
850	15.41	3.74	–	850	γCHI
839	6.48	4.50	835	840	γCHIII
816	24.57	12.17	815	816	δNO_2
790	10.78	11.73	788	792	γCHIII
777	36.82	22.04	770	777	γCHII
747	1.59	4.10	–	750	δNO_2
745	40.43	2.20	747	–	γCHIII
731	95.77	0.51	735	734	δNO_2
720	10.85	8.47	–	718	τPhIII
683	16.17	6.88	–	690	τPhI
675	11.42	18.21	673	–	δPhII
660	9.20	28.25	–	660	δPhI
630	18.46	13.29	–	632	γNH
612	11.54	19.50	–	614	δPhIII
582	5.27	8.15	–	582	τPhII
563	8.67	8.05	–	561	δNO_2
508	4.06	3.42	–	506	δNO_2
472	0.66	1.16	–	472	δPhII
428	7.15	1.85	–	427	τPhII
418	12.86	1.29	–	416	τPhI
390	6.92	5.80	–	391	τNO_2
338	10.63	3.09	–	338	τSO_2
326	1.26	2.36	–	324	τNO_2

(continued)

Table 1. Continued.

B3LYP/CC-pVDZ $\nu(\text{cm}^{-1})$	IR IRI	RA	$\nu(\text{cm}^{-1})$	Raman $\nu(\text{cm}^{-1})$	Assignments –
291	0.55	6.13	–	293	τ PhIII
260	0.48	2.06	–	261	τ SO2
243	0.15	1.27	–	240	τ CH2
NO2 ==I					
Benzo=====II					
Chlor=====III					
FBPS					
3396	107.93	–	3200	–	ν NH
3109	8.59	30.68	3109	–	ν CHI
3064	9.25	6.84	3062	–	ν CHIII
3000	2.77	8.87	3000	–	ν CH2
2950	12.01	15.16	2945	–	ν CH2
1613	18.69	16.79	–	1620	ν NO2
1604	31.26	3.28	1604	–	ν PhIII
1595	10.82	156.9	–	1595	ν PhII
1585	8.31	7.88	1586	–	ν PhIII
1558	11.23	238.2	–	1560	ν C = N
1556	94.32	24.68	1554	1550	ν NO2
1497	127.9	1.58	1502	–	ν PhIII
1454	158.67	38.18	1455	–	ν PhII
1422	8.94	27.28	1420	1424	δ CH2
1403	3.71	0.45	–	1406	ν PhIII
1343	383.1	156.0	1345	1343	ν NO2
1323	71.29	3.46	1325	–	ν PhI
1283	7.58	2.95	1285	–	δ CH2
1269	67.71	6.74	1265	1270	ν SO2
1231	126.3	9.02	1229	1229	ν CF
1168	30.60	18.47	1168	1166	δ CHII
1127	5.47	67.71	–	1130	δ CHI
1099	52.86	8.41	1102	–	δ CHII
1096	6.73	7.04	–	1094	ν SO2
1080	6.81	2.88	1081	–	δ CHIII
1065	9.81	3.55	–	1057	δ CHI
1017	6.26	14.53	1012	1020	ν PhI
972	0.01	0.72	969	977	γ CHI
951	42.9	14.74	948	952	δ CH2
926	24.89	3.47	925	–	ν CO
912	12.89	2.10	–	912	γ CHI
910	1.08	1.06	909	–	γ CHII
861	73.72	37.8	859	860	γ CHII
838	5.23	4.78	840	–	γ CHIII
832	5.38	47.58	831	833	ν PhIII
800	1.10	4.32	803	801	γ CHIII
780	34.46	9.68	778	775	γ CHII
747	1.08	3.53	747	745	δ NO2
732	94.65	0.40	731	–	δ NO2
660	100.6	16.48	661	662	τ PhII
643	2.56	12.07	–	640	δ PhI
622	1.32	7.60	–	620	δ PhII
587	5.06	13.20	–	588	γ NH
508	6.07	2.99	–	508	δ SO2
469	6.22	3.04	–	471	δ NO2
436	3.29	5/19	–	438	δ PhI
393	4.44	3.23	–	390	τ NH
361	1.83	2.34	–	359	τ PhI
334	1.17	5.13	–	335	τ NO2
305	5.01	0.53	–	307	τ CH2
269	0.86	0.41	–	267	τ SO2
214	2.16	3.88	–	225	τ PhIII
Nitr=====I					
Benzo——II					
Flurint =====III					

do not show any change in the amount and stability during the cell cycle, the protein level of topoisomerase II α varies depending on the position of the cell cycle and the proliferation step. This particular behavior of topoisomerase II α has made this enzyme a priority cellular target for various antineoplastic drugs, and these antineoplastic drugs show more lethal action against cells with high DNA replication rate and also with high topoisomerase II levels. Topo II inhibitors cause double-chain breaks in DNA, while Topo I inhibitors cause single-chain breaks. However, DNA single-chain fractures induced by Topo I inhibitors are probably converted to double-chain forties if they occur only in the continuous chain during replication. So, such drugs turn the Topo I molecule into an agent that damages DNA.^{25,26} Additionally, we are planning to examine the effects of these compounds on Topo II alpha as future study for more information. Crystal structure of Human Topoisomerase II enzyme binds with inhibitor, and etoposide was taken from the Protein Data Bank with ID: 5GWK.²⁷ Prior to docking of the ligands in the active site of the protein, preparation was performed on protein using protein preparation wizard of the software. All hetero atoms and water molecules were removed during the protein preparation followed by the addition of hydrogen atoms. Then, the active site of protein was well defined for the generation of the grid. The grid box was limited to the size of 20 Å at the active site. After that, docking studies were performed with Grid-based Ligand Docking with Energetics (GLIDE) module of this suite, the ligands were docked into the prepared grid by using “Standard precision mode,” and no constraints were defined. The docking method was first validated by docking of the known inhibitor, etoposide with 0.42 Å RMSD (root-mean-square deviation) value. To evaluate the receptors active site spatial fit, favorable ligand conformations were generated. The best fitted conformations of the ligands were evaluated and minimized for generating glide scores. To predict the binding affinities and best alignment of the compounds at the active site of the enzyme, hydrogen bonds and pi interactions formed with the surrounding amino acids and glide scores were used. The docking score is -8.040, -7.067, -6.724, and -10.193 for PTPS, CNSB, FBPS, and etoposide, respectively. According to the docking results, PTPS showed strong interactions between one of the important active site residues, Arg487 and DNA similar to etoposide with the docking score of -8.040. PTPS also revealed pi-pi stacking with deoxycytidine DC8, deoxyadenosine DA12, and deoxyguanosin DG13. CNSB revealed H-bond and salt bridges with Arg487; pi-pi stacking and pi-cation interactions with deoxyguanosin DG13. FBPS revealed H-bonds with deoxyadenosine DA6 and deoxycytidine DC8. The compounds used in this manuscript can be used for the design of potent inhibitory drugs of Topoisomerase II enzyme, as lead compounds (Figure 4). Fig S1(Supplementary Information) gives the three-dimensional pictures.

Molecular electrostatic potential (MEP)

MEP provides information about the overall electronic distribution in a particular compound. The color code used provides information of the electron distribution. Usually, the red colored region represents electronegative regions, in the title compounds, and it is found especially near oxygen atoms and nitrogen atoms, and represents the nucleophilic area of the molecules, which is capable of forming stabilizing interactions such as hydrogen bond and other electrostatic bonds with neighboring molecules or solvent molecules in the condensed phase (Figure 5).^{28,29} Electrophilic regions are found near carbon atoms, indicated by blue color. The presence of both electrophilic and nucleophilic is in the molecule shows that there is a possibility of high degree of electrostatic interactions in the molecule in the condensed state, making the three molecules as ideal candidates for using as drugs. This difference in electronic arrangement is vital in the exhibition of several useful physical and chemical phenomena such as NLO activity, which is explained in the next section.

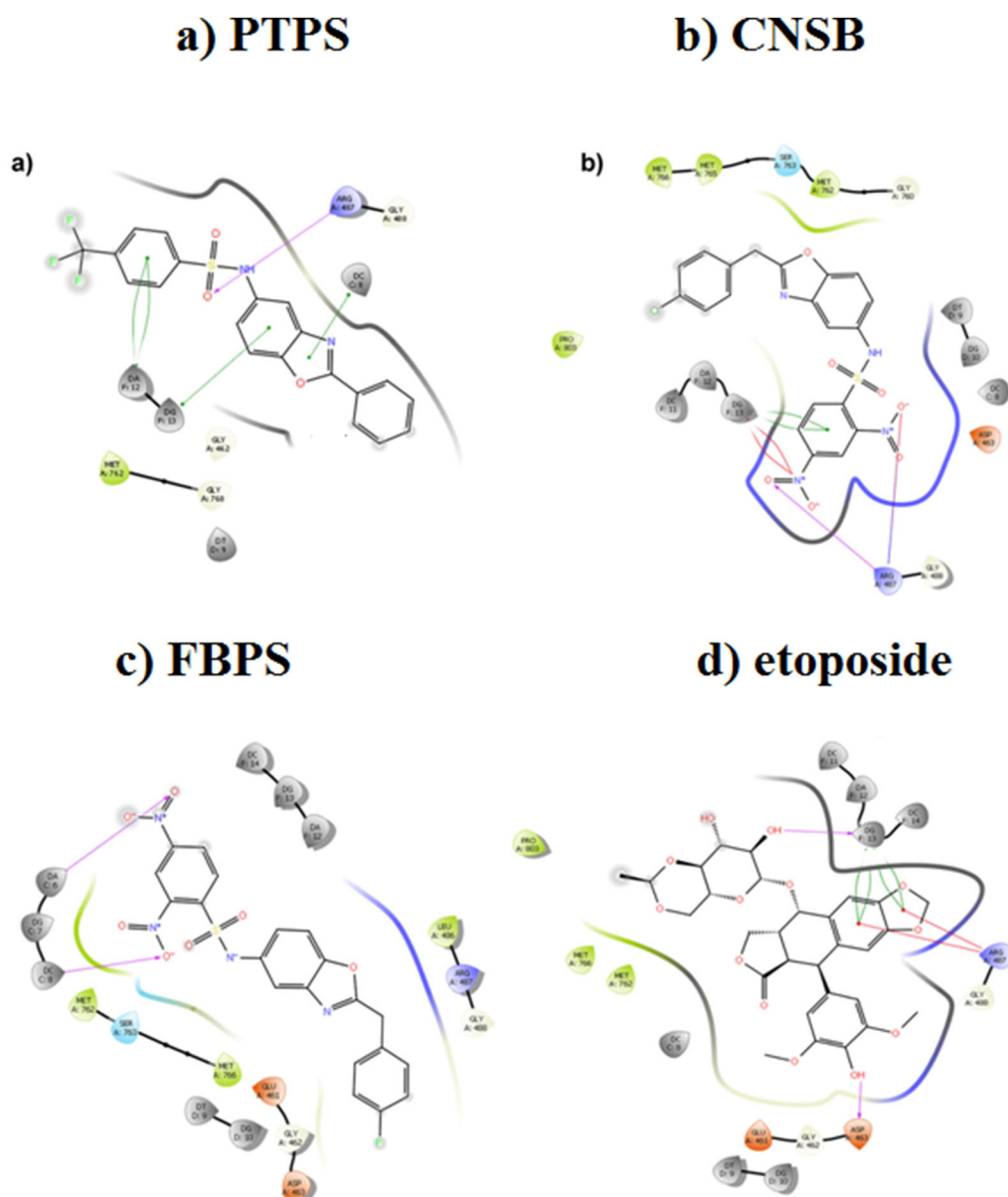


Figure 4. a) Docked position of PTPS: Compound revealed H-bond with Arg487; pi-pi stacking with deoxycytidine DC8, deoxyadenosine DA12, and deoxyguanosin DG13. b) Docked position of cnsb: Compound revealed H-bond and salt bridge with Arg487; pi-pi stacking; and pi-cation interactions with deoxyguanosin DG13. c) Docked position of FBPS: compound revealed H-bonds with deoxyadenosine DA6 and deoxycytidine DC8. d) Docked position of etoposide: Compound revealed H-bond with deoxyguanosin DG13, and Asp463; pi-pi stacking with deoxyguanosin DG13; pi-cation interactions with Arg487. Pink color line refers to H bond. Green color line refers to pi-pi interaction. Red color line refers to pi-cation interaction.

Nonlinear optical (NLO) properties of the molecules

The molecules may differ in their response to a strong light/optical field. Some materials may deviate the path of the light from their usual linear pattern and is termed as the nonlinear behavior.³⁰ This behavior is very important during the design of several electronic devices such as logical gates, communication devices, light switches, memory devices. Theoretically, this NLO ability can be modeled using the hyperpolarizability values obtained from the calculations of

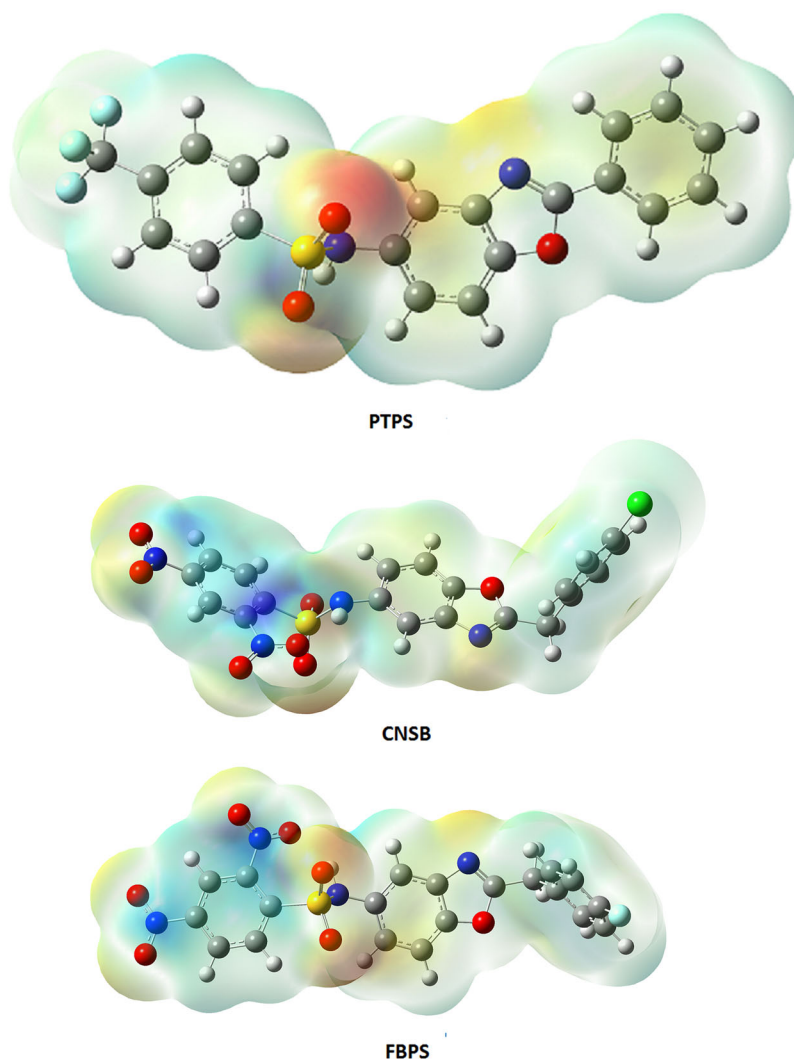


Figure 5. MESP plots of the compounds to identify electrophilic and nucleophilic centers.

Raman spectra during frequency calculations. The calculated data of α and β are represented in Table 2. Data indicate first-order hyperpolarizability (β_{zyy} and β_{yyy} for PTPS, β_{yyy} and β_{xyy} for CNSB, and β_{xxy} and β_{xxx} for FBPS) is larger compared to other positive and negative values in the hyperpolarizability data. Difference in electronic distribution is responsible for this change. The title molecules are therefore highly polarized due to the donor-to-acceptor π -electron transfer. It is a common habit to compare the NLO values with the standard urea molecule, which is usually used as a reference. The study indicated that the molecules PTPS, CNSB, and FBPS show first-order hyperpolarizability value which is 20.33, 114.48, and 114.18 times greater than urea. Hence, the three compounds can be used for the preparation of standard NLO materials.

Natural bond orbital (NBO) analysis

NBO analysis is performed using the NBO suite incorporated in the Gaussian09 software. This study is used to determine various intra-molecular interactions such as hyperconjugation effect

Table 2. Calculated hyperpolarizability and polarizability components.

	PTPS	CNSB	FBPS
A			
β_{xxx}	21.267	-426.0796	-558.5837
β_{xxy}	61.6787	429.944	675.8251
β_{xyy}	-41.5645	-622.3115	-544.1882
β_{yyy}	-300.7555	830.6251	446.6925
β_{zxx}	-19.1115	233.5987	158.2589
β_{xyz}	-0.0065	-26.3195	144.5777
β_{zyy}	122.8723	-51.9927	-177.5535
β_{xzz}	0.4975	-80.3863	-81.3845
β_{yzz}	-37.4266	7.0027	115.0023
β_{zzz}	25.5494	113.2188	-116.5221
a			
α_{xx}	197.1956	323.9428	326.8937
α_{xy}	-71.5587	-104.559	-91.4877
α_{yy}	429.3164	327.923	351.3421
α_{xz}	-58.3440	-11.7996	34.7819
α_{yz}	-38.2214	51.1627	-13.8035
α_{zz}	178.3933	246.0685	179.5972

present in the molecules of interest. For the compounds under study, the NBO values are presented in the Table 3. For the title molecules, the interactions due to oxygen atoms in the SO₂ group are as follows: LPO12→σ*(C3-S11) is 20.17, LPO12→σ*(O13-S11) is 15.70, LPO12→σ*(N14-S11) is 21.52, LPO13→σ*(C3-S11) is 19.19, LPO13→σ*(O12-S11) is 16.14, LPO13→σ*(N14-S11) is 21.19 kcal/mol for PTPS; LPO9→σ*(C3-S8) is 22.21, LPO9→σ*(S8-O10) is 12.78, LPO9→σ*(S8-N11) is 25.44, LPO10→σ*(S8-O9) is 16.63, LPO10→σ*(S8-N11) is 19.06, LPO10→σ*(C3-S8) is 22.63 kcal/mol for CNSB and LPO10→σ*(S8-O9) is 16.60, LPO10→σ*(S8-N11) is 19.12, LPO10→σ*(S8-C3) is 22.67, LPO9→σ*(S8-N11) is 25.41, LPO9→σ*(S8-O10) is 12.77, LPO10→σ*(S8-C3) is 22.21 kcal/mol for FBPS. Due to benzoxazole oxygen atom, the interactions are as follows: LPO21→π*(C17-C18) is 24.22, LPO21→π*(C22-N23) is 34.02 kcal/mol for PTPS; LPO18→π*(C14-C15) is 24.31, LPO18→π*(C19-N20) is 35.40 for CNSB and LPO18→π*(C14-C15) is 24.39, LPO18→π*(C19-N20) is 35.34 for FBPS. Nitro oxygen atom interactions are as follows: LPO21→σ*(N7-O22) is 19.26, LPO22→σ*(N7-O21) is 19.19, LPO22→π*(N7-O21) is 167.06, LPO32→σ*(C4-N31) is 14.04, LPO32→σ*(N31-O33) is 19.84, LPO33→σ*(N31-O32) is 19.74, LPO33→π*(N31-O32) is 153.04 for CNSB and LPO33→π*(N31-O32) is 153.24, LPO33→σ*(N31-O32) is 19.74, LPO22→π*(N7-O21) is 167.06 for FBPS. The other major interactions are as follows: LPF8→σ*(C7-F10) is 12.77, LPF9→σ*(C7-F8) is 11.54, LPF9→σ*(C7-F10) is 11.48, LPF10→σ*(C7-F8) is 12.76, LPN23→σ*(O21-C22) is 14.27 (PTPS), and LPN20→σ*(C19-O18) is 14.40 (CNSB). The results indicate a variety of hyperconjugate interactions in the molecule itself, which stabilizes the molecule to higher extent. Also, this suggests the intermolecular charge transfer (ICT) possible in the molecules.

The frontier molecular orbitals

The molecular orbital theory is commonly used by chemists to evaluate the reactivity and stability of the compounds.³¹ The frontier molecular orbitals, HOMO and LUMO, play a very important role in this evaluation. More the energy difference between HOMO and LUMO, the band gap will be wide and molecule will be more stable comparatively. The LUMO energy of PTPS, CNSB, and FBPS is -5.295/-5.091/-5.091 eV and HOMO energy of PTPS, CNSB, and FBPS is -8.272/-8.077/-8.288 eV. The energy gap of molecules PTPS, CNSB, and FBPS is found to be 2.977, 2.986, and 3.197 eV, respectively. Figure 6 shows the HOMO and LUMO map of the molecules PTPS, CNSB, and FBPS. Table 4 contains the calculated chemical hardness of molecules PTPS, CNSB, and FBPS. The results indicate that molecule FBPS is harder and less reactive than

Table 3. Second-order perturbation theory analysis of Fock matrix in NBO basis corresponding to the intra-molecular bonds of the title compound.

Donor	Type	ED/e	Acceptor	Type	ED/e	E(2) ^a	E(j)-E(i) ^b	F(i,j) ^c
3.1. PTPS								
LPF8	π	1.94842	C6-C7	σ^*	0.06272	6.65	0.78	0.065
-	π	1.94842	C7-F9	σ^*	0.11178	6.11	0.65	0.057
-	π	1.94842	C7-F10	σ^*	0.10229	3.53	0.64	0.043
-	n	1.93059	C7-F9	σ^*	0.11178	9.92	0.65	0.072
-	n	1.93059	C7-F10	σ^*	0.10229	12.77	0.64	0.082
LPF9	π	1.94588	C6-C7	σ^*	0.06272	6.69	0.78	0.065
-	π	1.94588	C7-F8	σ^*	0.10312	4.75	0.64	0.050
-	π	1.94588	C7-F10	σ^*	0.10229	4.83	0.64	0.050
-	n	1.92959	C7-F8	σ^*	0.10312	11.54	0.64	0.077
-	n	1.92959	C7-F10	σ^*	0.10229	11.48	0.64	0.077
LPF10	π	1.94825	C6-C7	σ^*	0.06272	6.66	0.78	0.065
-	π	1.94825	C7-F8	σ^*	0.10312	3.54	0.64	0.043
-	π	1.94825	C7-F9	σ^*	0.11178	6.11	0.65	0.057
LPF10	n	1.93073	C7-F8	σ^*	0.10312	12.76	0.64	0.082
-	n	1.93073	C7-F9	σ^*	0.11178	9.96	0.65	0.072
LPO12	σ	1.98129	S11-O13	σ^*	0.16629	1.69	1.06	0.039
-	π	1.79616	C3-S11	σ^*	0.20558	20.17	0.44	0.084
-	π	1.79616	S11-O13	σ^*	0.16629	7.34	0.56	0.058
-	π	1.79616	S11-N14	σ^*	0.28523	5.25	0.39	0.041
-	n	1.78994	S11-O13	σ^*	0.16629	15.70	0.56	0.085
-	n	1.78994	S11-N14	σ^*	0.28523	21.52	0.39	0.083
LPO13	σ	1.98043	S11-O12	σ^*	0.14320	1.83	1.07	0.041
-	π	1.80557	C3-S11	σ^*	0.20558	19.19	0.44	0.082
-	π	1.80557	S11-O12	σ^*	0.14320	5.80	0.57	0.052
-	π	1.80557	S11-N14	σ^*	0.28523	6.66	0.39	0.047
-	n	1.78052	S11-O12	σ^*	0.14320	16.14	0.57	0.087
-	n	1.78052	S11-N14	σ^*	0.28523	21.19	0.39	0.082
LPN14	σ	1.89289	C3-S11	σ^*	0.20558	1.86	0.49	0.028
-	σ	1.89289	S11-O13	σ^*	0.16629	7.74	0.62	0.063
-	σ	1.89289	C15-C16	σ^*	0.02168	1.57	0.91	0.035
-	σ	1.89289	C15-C16	π^*	0.35754	4.91	0.37	0.041
-	σ	1.89289	C15-C20	σ^*	0.02545	5.36	0.89	0.063
LPO21	σ	1.96929	C17-C18	σ^*	0.04129	3.59	1.13	0.057
-	σ	1.96929	C22-N23	σ^*	0.01730	4.98	1.16	0.068
-	π	1.73018	C17-C18	π^*	0.45618	24.22	0.36	0.088
-	π	1.73018	C22-N23	π^*	0.30492	34.02	0.35	0.098
LPN23	σ	1.91104	C17-C18	σ^*	0.04129	6.17	0.91	0.068
-	σ	1.91104	O21-C22	σ^*	0.06274	14.27	0.69	0.089
3.2. CNSB								
LPO9	σ	1.97872	S8-O10	σ^*	0.14183	1.94	1.07	0.042
-	π	1.78913	C3-S8	σ^*	0.23652	22.21	0.40	0.085
-	π	1.78913	S8-O10	σ^*	0.14183	9.34	0.56	0.066
-	π	1.78913	S8-N11	σ^*	0.26596	2.29	0.41	0.028
LPO9	n	1.77181	S8-O10	σ^*	0.14183	12.78	0.56	0.077
-	n	1.77181	S8-N11	σ^*	0.26596	25.44	0.41	0.092
LPO10	σ	1.98055	S8-O9	σ^*	0.17055	1.53	1.07	0.038
-	π	1.80708	S8-O9	σ^*	0.17055	16.63	0.57	0.087
-	π	1.80708	S8-N11	σ^*	0.26596	19.06	0.41	0.081
-	n	1.78726	C3-S8	σ^*	0.23652	22.63	0.41	0.086
-	n	1.78726	S8-O9	σ^*	0.17055	5.57	0.57	0.051
-	n	1.78726	S8-N11	σ^*	0.26596	5.26	0.41	0.042
LPN11	σ	1.86752	C3-S8	σ^*	0.23652	2.69	0.44	0.032
-	σ	1.86752	S8-O9	σ^*	0.17055	9.58	0.61	0.069
-	σ	1.86752	C12-C13	σ^*	0.02202	4.72	0.90	0.060
-	σ	1.86752	C12-C13	π^*	0.36823	6.74	0.36	0.047
-	σ	1.86752	C12-C17	σ^*	0.02406	1.73	0.89	0.036
LPO18	σ	1.96999	C14-C15	σ^*	0.04042	3.56	1.13	0.057
-	σ	1.96999	C19-N20	σ^*	0.02020	5.15	1.17	0.069
-	π	1.72382	C14-C15	π^*	0.44883	24.31	0.36	0.087
-	π	1.72382	C19-N20	π^*	0.25974	35.40	0.35	0.099

(continued)

Table 3. Continued.

Donor	Type	ED/e	Acceptor	Type	ED/e	E(2) ^a	E(j)-E(i) ^b	F(i,j) ^c
LPN20	σ	1.91326	C14-C15	σ^*	0.04042	5.99	0.91	0.067
-	σ	1.91326	O18-C19	σ^*	0.06887	14.40	0.69	0.090
LPO21	σ	1.98068	C6-N7	σ^*	0.11109	4.21	1.06	0.061
-	σ	1.98068	N7-O22	σ^*	0.05652	2.66	1.22	0.051
-	π	1.89384	C6-N7	σ^*	0.11109	13.64	0.55	0.078
-	π	1.89384	N7-O22	σ^*	0.05652	19.26	0.71	0.106
LPO22	σ	1.98071	C6-N7	σ^*	0.11109	4.19	1.06	0.061
-	σ	1.98071	N7-O21	σ^*	0.05657	2.67	1.22	0.051
-	π	1.89408	C6-N7	σ^*	0.11109	13.55	0.55	0.077
-	π	1.89408	N7-O21	σ^*	0.05657	19.19	0.71	0.106
-	n	1.43163	N7-O21	π^*	0.61775	167.06	0.14	0.140
LPCI30	σ	1.99339	C26-C27	σ^*	0.02646	1.26	1.48	0.039
-	σ	1.99339	C27-C28	σ^*	0.02669	1.25	1.47	0.038
-	π	1.97315	C26-C27	σ^*	0.02646	3.85	0.88	0.052
-	π	1.97315	C27-C28	σ^*	0.02669	3.85	0.87	0.052
-	n	1.93162	C26-C27	π^*	0.38348	12.07	0.33	0.061
LPO32	σ	1.98060	C4-N31	σ^*	0.10768	4.17	1.06	0.061
-	σ	1.98060	N31-O33	σ^*	0.06996	2.77	1.20	0.052
-	π	1.88851	C4-N31	σ^*	0.10768	14.04	0.55	0.079
-	π	1.88851	N31-O33	σ^*	0.06996	19.84	0.69	0.106
LPO33	σ	1.97348	C4-N31	σ^*	0.10768	5.00	1.05	0.066
-	σ	1.97348	N31-O32	σ^*	0.05850	1.73	1.21	0.041
-	π	1.89375	C4-N31	σ^*	0.10768	11.00	0.56	0.070
-	π	1.89375	N11-H37	σ^*	0.02608	3.76	0.78	0.049
-	π	1.89375	N31-O32	σ^*	0.05850	19.74	0.72	0.108
-	n	1.44727	N31-O32	π^*	0.58799	153.04	0.16	0.140
-	n	1.44727	N31-O33	σ^*	0.06996	5.69	0.69	0.064
3.3. FBPS								
C3-S8	σ	1.96026	S8-O9	σ^*	0.17063	3.51	0.96	0.054
S8-O10	σ	1.98380	S8-O9	σ^*	0.17063	2.17	1.26	0.049
-			S8-N11	σ^*	0.26589	2.17	1.10	0.047
S8-N11	σ	1.96410	S8-O9	σ^*	0.17063	3.52	1.03	0.056
-			S8-O10	σ^*	0.14173	3.33	1.03	0.054
S8-O9	σ	1.98146	S8-N11	σ^*	0.26589	2.72	1.10	0.052
C12-C13	σ	1.97411	C14-N20	σ^*	0.02054	5.54	1.16	0.072
C14-C15	σ	1.97626	C15-C16	σ^*	0.02124	4.36	1.28	0.067
-	π	1.60854	C12-C13	π^*	0.36881	19.68	0.29	0.067
-			C16-C17	π^*	0.32553	18.73	0.29	0.067
-			C19-N20	π^*	0.25929	9.96	0.27	0.048
C19-N20	σ	1.98680	C13-C14	σ^*	0.02223	5.84	1.45	0.082
-	π	1.88730	C14-C15	π^*	0.04048	15.54	0.35	0.072
O18-C19	σ	1.98911	C15-C16	σ^*	0.02124	5.01	1.47	0.077
N7-O21	π	1.98467	N7-O21	π^*	0.61785	7.25	0.32	0.052
C26-C27	π	1.98032	C24-C25	π^*	0.35399	20.68	0.30	0.070
-			C28-C29	π^*	0.32944	18.68	0.29	0.066
C27-C28	σ	1.98246	C26-C27	σ^*	0.02744	3.30	1.28	0.058
N31-O32	π	1.98520	N31-O32	π^*	0.58815	6.54	0.34	0.050
LPO9	π	1.78923	C3-S8	σ^*	0.23670	22.21	0.40	0.085
-			S8-O10	σ^*	0.14173	9.34	0.56	0.066
-	n	1.77217	S8-O10	σ^*	0.14173	12.77	0.56	0.077
-			S8-N11	σ^*	0.26589	25.41	0.41	0.092
LPO10	π	1.80689	S8-O9	σ^*	0.17063	16.60	0.57	0.087
-			S8-N11	σ^*	0.26589	19.12	0.41	0.081
-	n	1.78710	C3-S8	σ^*	0.23670	22.67	0.41	0.086
-			S8-O9	σ^*	0.17063	5.62	0.57	0.051
-			S8-N11	σ^*	0.26589	5.22	0.41	0.042
LPN11	σ	1.86893	S8-O9	σ^*	0.17063	9.57	0.61	0.069
-	-		C12-C13	π^*	0.36881	6.39	0.36	0.046
LPO18	π	1.72380	C14-C15	π^*	0.44876	24.39	0.36	0.087
-	-		C19-N20	π^*	0.25929	35.34	0.35	0.099
LPN20	Σ	1.91318	C14-C15	σ^*	0.04048	6.00	0.91	0.067
-	-		O18-C19	σ^*	0.06899	14.40	0.69	0.090

(continued)

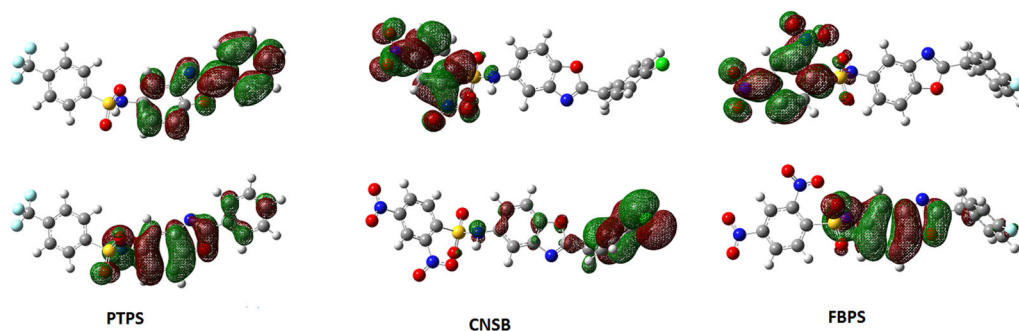
Table 3. Continued.

Donor	Type	ED/e	Acceptor	Type	ED/e	E(2) ^a	E(j)-E(i) ^b	F(i,j) ^c
LPO21	π	1.98068	C6-N7	σ^*	0.11103	13.63	0.55	0.078
-			N7-O22	σ^*	0.05651	19.25	0.71	0.106
LPO22	π	1.89413	C6-N7	σ^*	0.11103	13.54	0.55	0.077
-			N7-O21	σ^*	0.05658	19.20	0.71	0.106
	n	1.43167	N7-O21	π^*	0.61785	167.06	0.14	0.140
LPF30	π	1.96802	C26-C27	σ^*	0.02744	6.59	0.96	0.071
-			C27-C28	σ^*	0.02767	6.60	0.96	0.071
	n	1.91678	C26-C27	π^*	0.37030	20.33	0.42	0.089
LPO32	π	1.88855	C4-N31	σ^*	0.10768	14.03	0.55	0.079
			N31-O33	σ^*	0.06999	19.83	0.69	0.106
LPO33	π	1.89373	C4-N31	σ^*	0.10768	11.02	0.56	0.070
			N31-O32	σ^*	0.05854	19.74	0.72	0.108
	n	1.44694	N31-O32	π^*	0.58815	153.24	0.16	0.140

^aE(2) means energy difference of hyper-conjugative interactions (stabilization energy in kJ/mol).

^bEnergy difference (a.u.) between donor and acceptors i and j NBO orbitals.

^cF(i,j) is the Fock matrix elements (a.u.) between i and j NBO orbitals.

**Figure 6.** Frontier MO's of the compounds.**Table 4.** The calculated global reactivity properties from DFT.

Global reactivity descriptors	Energy (eV)		
	PTPS	TCNSB	FBPS
HOMO energy	-8.272	-8.077	-8.288
LUMO energy	-5.295	-5.091	-5.091
Band gap	2.977	2.986	3.197
Ionization potential $I = -E_{\text{HOMO}}$	8.272	8.077	8.288
Electron affinity $A = -E_{\text{LUMO}}$	5.295	5.091	5.091
$\mu = -(I + A)/2$	-6.784	-6.584	-6.690
Global hardness $\eta = (I - A)/2$	1.489	1.493	1.599
Electrophilicity $\omega = \mu^2/2\eta$	15.454	14.517	13.995
Electro negativity $\chi = (I + A)/2$	6.784	6.584	6.690

molecules PTPS and CNSB. The computed electronegativity (χ) values for the molecules PTPS (6.784), CNSB (6.584), and FBPS (6.690) are given in Table 4. FBPS has higher electronegativity than PTPS and CNSB. The electrophilicity values for the molecules PTPS, CNSB, and FBPS were found to be 15.454, 14.517, and 13.995 eV as shown in Table 4. Among the molecules, FBPS is maximum nucleophile, while PTPS is maximum electrophile. The ionization potential and electron affinity of molecules calculated in gas phase values are 8.272/5.295, 8.077/5.091, and 8.288/5.091 eV, respectively.

Light harvesting studies

Light harvesting efficiency studies can be used to screen whether an organic compound can be used as a photosensitizer to convert light energy into electric energy in a dye-sensitized solar cell. This is determined from the electronic spectral analysis, which is generated by time-dependent DFT analysis using CAM-B3LYP functional using CC-pVDZ basis set. Oscillator strength corresponding to λ_{\max} can provide a direct link between the electronic spectra and LHE as $\text{LHE} = 1 - 10^{-f}$, where f is the oscillator strength.^{32–34} For PTPS, λ_{\max} is 287.12 nm, $f = 1.1824$, and $\text{LHE} = 0.9342$. For CNSB, λ_{\max} is 314.65 nm, $f = 0.0001$, and $\text{LHE} = 0.0023$. For FBPS, λ_{\max} is 314.7 nm, $f = 0.0001$, and $\text{LHE} = 0.0023$. The second and third compounds contain halogen, which is an electron-withdrawing group attached to the phenyl ring which is linked to the benzoxazole moiety.^{34,35–38} This may hamper the LHE of CNSB and FBPS. LHE of PTPS is 0.9342 means that the dye can transfer 93.42% of light energy to electrical energy and this can be used along with other dyes which are presently used as photosensitizers in DSSC's.

Conclusions

Geometry of the molecules under study was explained using the experimental and theoretical methods. Scaled IR and Raman spectra show good agreement with the experimental spectra followed by vibrational assignment. MESP gives information about the electronic distribution, and it is found that they are not uniformly distributed in the molecules of our study, paving the way to show excellent physico-chemico and optical properties. Hyperpolarizability studies provide the NLO data, and it is found that all the three molecules are having exceptionally good NLO properties compared to the standard materials. According to molecular docking studies, the three sulfonamidobenzoxazoles can be useful in designing of new potent inhibitors of Topoisomerase II enzyme, as lead compounds. Light harvesting studies of the compounds are reported. LHE of PTPS is 0.9342 means that the dye can transfer 93.42% of light energy to electrical energy and this can be used along with other dyes which are presently used as photosensitizers in DSSC's.

ORCID

Renjith Thomas  <http://orcid.org/0000-0003-0011-633X>

References

1. M. Prudhomme, J. Guyot, and G. Jeminet, "Semi-Synthesis of A23187 (Calcimycin) Analogs. IV. Cation Carrier Properties in Mitochondria of Analogs with Modified Benzoxazole Rings. Antimicrobial Activity," *The Journal of Antibiotics* 39, no. 7 (1986): 934–37.
2. I. Yildiz-Oren, B. Tekiner-Gulbas, I. Yalcin, O. Temiz-Arpaci, E. Aki-Sener, and N. Altanlar, "Synthesis and Antimicrobial Activity of New 2-[p-Substituted-Benzyl]-5-[Substituted-Carbonylamino]Benzoxazoles," *Archiv Der Pharmazie* 337, no. 7 (2004): 402–10.
3. T. Ertan-Bolelli, K. Bolelli, Y. Musdal, I. Yildiz, E. Aki-Yalcin, B. Mannervik, and I. Yalcin, "Design and Synthesis of 2-Substituted-5-(4-Trifluoromethyl Phenyl Sulphonamido) Benzoxazole Derivatives as Human GST P1-1 Inhibitors," *Artificial Cells, Nano Medicine, and Biotechnology* 46, no. 3 (2018): 510–17.
4. T. Ertan-Bolelli, I. Yildiz, and S. Ozgen-Ozgacar, "Synthesis, Molecular Docking and Antimicrobial Evaluation of Novel Benzoxazole Derivatives," *Medicinal Chemistry Research* 25, no. 4 (2016): 553–67.
5. T. Ertan-Bolelli, K. Bolelli, S. Okten, F. Kaynak-Onurdag, E. Aki-Yalcin, and I. Yalcin, "Synthesis, Antimicrobial Activities of New Sulfonamidobenzoxazoles and Molecular Docking Studies on *Escherichia coli* TEM-1 β -Lactamase," *Croatica Chemica Acta* 90, no. 1 (2017): 67–74.
6. M. Yamashita, T. Tahara, S. Hayakawa, H. Matsumoto, S.-I. Wada, K. Tomioka, and A. Iida, "Synthesis and Biological Evaluation of Histone Deacetylase and DNA Topoisomerase II-Targeted Inhibitors," *Bioorganic & Medicinal Chemistry* 26, no. 8 (2018): 1920–28.

7. Y. Sheena Mary, Nourah Z. Alzoman, Vidya V. Menon, Ebtehal S. Al-Abdullah, Ali A. El-Emam, C. Yohannan Panicker, Ozlem Temiz-Arpaci, Stevan Armaković, Sanja J. Armaković, and C. Van Alsenoy, "Reactive, Spectroscopic and Antimicrobial Assessments of 5-[(4-Methylphenyl)Acetoxy]-2-(4-Tert-Butylphenyl)Benzoxazole: Combined Experimental and Computational Study," *Journal of Molecular Structure* 1128 (2017): 694–706.
8. V. V. Aswathy, Sabiha Alper-Hayta, Gözde Yalcin, Y. Sheena Mary, C. Yohannan Panicker, P. J. Jojo, Fatma Kaynak-Onurdag, Stevan Armaković, Sanja J. Armaković, Ilkay Yildiz, et al. "Modification of Benzoxazole Derivative by Bromine-Spectroscopic, Antibacterial and Reactivity Study Using Experimental and Theoretical Procedures," *Journal of Molecular Structure* 1141 (2017): 495–511.
9. Asha Chandran, Hema Tresa Varghese, Y. Sheena Mary, C. Yohannan Panicker, T. K. Manojkumar, Christian Van Alsenoy, and G. Rajendran, "FT-IR, FT-Raman and Computational Study of (E)-N-Carbamidoyl-4-((4-Methoxybenzylidene)Amino)Benzene Sulfonamide," *Spectrochimica Acta Part A: Molecular and Biomolecular Spectroscopy* 92 (2012): 84–90.
10. A. Chandran, Y. S. Mary, H. T. Varghese, C. Y. Panicker, P. Pazdera, G. Rajendran, and N. Babu, "FT-IR, FT-Raman Spectroscopy and Computational Study of N-Carbamidoyl-4-[(E)-((2-Hydroxyphenyl)Methylidene)Amino] Benzenesulfonamide," *Journal of Molecular Structure* 992, no. 1–3 (2011): 77–83.
11. P. Shafieyoon, E. Mehdipour, and Y. S. Mary, "Synthesis, Characterization and Biological Investigation of Glycine-Based Sulfonamide Derivative and Its Complex: Vibration Assignment, HOMO-LUMO Analysis, MEP and Molecular Docking," *Journal of Molecular Structure* 1181 (2019): 244–52.
12. R. G. Parr, and W. Yang, *Density-Functional Theory of Atoms and Molecules, International Series of Monographs on Chemistry* (New York: Oxford Science Publications, 1995).
13. W. Koch, and M. C. Holthausen, *A Chemist's Guide to Density Functional Theory* (Verlag: Wiley, 2001), 239–263.
14. G. M. Wynne, S. P. Wren, P. D. Johnson, P. D. Price, O. De Moor, G. Nugent, R. Storer, R. J. Pye, and C. R. Dorgan, *Treatment of Duchenne Muscular Dystrophy* (US Patent 8,518,980 B2, August 27, 2013).
15. T. Ertan-Bolelli, Y. Musdal, K. Bolelli, S. Yilmaz, Y. Aksoy, I. Yildiz, E. Aki-Yalcin, and I. Yalcin, "Synthesis and Biological Evaluation of 2-Substituted-5-(4-Nitrophenylsulfonamido)Benzoxazoles as Human GST P1-1 Inhibitors and Description of the Binding Site Features," *Chemmedchem* 9, no. 5 (2014): 984–92.
16. G. M. Wynne, S. P. Wren, P. D. Johnson, P. D. Price, O. De Moor, G. Nugent, R. Storer, R. J. Pye, and C. R. Dorgan, "Treatment of Duchenne muscular dystrophy" (US Patent 2009-075938, filed Feb 9, 2007, and issued Mar 19, 2009).
17. R. Dennington, T. Keith, and J. Millam, *GaussView* (Version 5) (Shawnee Mission, KS: Semichem Inc., 2009).
18. M. J. Frisch, G. W. Trucks, H. B. Schlegel, G. E. Scuseria, M. A. Robb, J. R. Cheeseman, G. Scalmani, V. Barone, B. Mennucci, and G. A. Petersson, *Gaussian 09* (Revision B.01) (Wallingford CT: Gaussian Inc., 2010).
19. J. B. Foresman, *Exploring Chemistry with Electronic Structure Methods: A Guide to Using Gaussian*, edited by E. Frisch, 2nd ed. (Pittsburg, PA: Gaussian, 1996).
20. N. P. G. Roeges, *A Guide to the Complete Interpretation of Infrared Spectra of Organic Structures* (New York: Wiley, 1994).
21. Schrödinger, *Schrödinger Release 2018-2* (New York: LLC, 2018).
22. Richard A. Friesner, Jay L. Banks, Robert B. Murphy, Thomas A. Halgren, Jasna J. Klicic, Daniel T. Mainz, Matthew P. Repasky, Eric H. Knoll, Mee Shelley, Jason K. Perry, et al. "Glide: A New Approach for Rapid, Accurate Docking and Scoring: Method and Assessment of Docking Accuracy," *Journal of Medicinal Chemistry* 47, no. 7 (2004): 1739–49.
23. Schrödinger LLC. New York, USA: Schrodinger Inc., 2008. <http://www.schrodinger.com>. Accessed 2nd January, 2019.
24. F. Cortes, N. Pastor, S. Mateos, and I. Dominguez, "Roles of DNA Topoisomerases in Chromosome Segregation and Mitosis," *Mutation Research/Reviews in Mutation Research* 543 (2003): 59–66.
25. J. L. Nitiss, and J. C. Wang, "Mechanisms of Cell Killing by Drugs That Trap Covalent Complexes between DNA Topoisomerases and DNA," *Molecular Pharmacology* 50, no. 5 (1996): 1095–102.
26. A. K. McClendon, and N. Osheroff, "DNA Topoisomerase II, Genotoxicity, and Cancer," *Mutation Research/Fundamental and Molecular Mechanisms of Mutagenesis* 623, no. 1–2 (2007): 83–97.
27. Y. R. Wang, S. F. Chen, C. C. Wu, Y. W. Liao, T. S. Lin, K. T. Liu, Y. S. Chen, T. K. Li, T. C. Chien, and N. L. Chan, "Producing Irreversible Topoisomerase II-Mediated DNA Breaks by Site-Specific Pt (II)-Methionine Coordination Chemistry," *Nucleic Acids Research* 45, no. 18 (2017): 10861–71.
28. P. Politzer, J. S. Murray, and Z. Peralta-Inga, "Molecular Surface Electrostatic Potentials in Relation to Noncovalent Interactions in Biological Systems," *International Journal of Quantum Chemistry* 81 (2001): 676–84.

29. D. R. Roy, U. Sarkar, P. K. Chattaraj, A. Mitra, J. Padmanabhan, R. Parthasarathi, V. Subramanian, S. V. Damme, and P. Bultinck, "Analyzing Toxicity through Electrophilicity," *Molecular Diversity* 10, no. 2 (2006): 119–31.
30. Y. S. Mary, K. Raju, C. Y. Panicker, A. A. Al-Saadi, and T. Thiemann, "Molecular Conformational Analysis, Vibrational Spectra, NBO Analysis and First Hyperpolarizability of (2E)-3-(3-Chlorophenyl)Prop-2-Enoic Anhydride Based on Density Functional Theory Calculations," *Spectrochimica Acta Part A: Molecular and Biomolecular Spectroscopy* 131 (2014): 471–83.
31. K. Fukui, "Role of Frontier Orbitals in Chemical Reactions," *Science* 218, no. 4574 (1982): 747–54.
32. C. Curutchet and B. Mennucci, "Quantum Chemical Studies of Light Harvesting," *Chemical Reviews* 117, no. 2 (2017): 294–343.
33. D. A. Thadathil, S. Varghese, K. B. Akshaya, R. Thomas, and A. Varghese, "An Insight into Photophysical Investigation of (E)-2-Fluoro-N'-(1-(4-Nitrophenyl) Ethylidene)Benzohydrazide through Solvatochromism Approaches and Computational Studies," *Journal of Fluorescence* 29, no. 4 (2019): 1013–27. <https://doi.org/10.1007/s10895-019-02415-y>.
34. V. S. Kumar, Y. S. Mary, K. Pradhan, D. Brahman, Y. Mary, R. Thomas, M. S. Roxy, and C. Van Alsenoy, "Synthesis, Spectral Properties, Chemical Descriptors and Light Harvesting Studies of a New Bioactive Azo Imidazole Compound," *Journal of Molecular Structure* 1199 (2020): 127035. <https://doi.org/10.1016/j.molstruc.2019.127035>
35. S. Beegum, Y. S. Mary, Y. S. Mary, R. Thomas, S. Armaković, S. J. Armaković, J. Zitko, M. Dolezal, and C. Van Alsenoy, "Exploring the Detailed Spectroscopic Characteristics, Chemical and Biological Activity of Two Cyanopyrazine-2-Carboxamide Derivatives Using Experimental and Theoretical Tools," *Spectrochimica Acta Part A: Molecular and Biomolecular Spectroscopy* 224 (2020): 117414. <https://doi.org/10.1016/j.saa.2019.117414>.
36. Y. Sheena Mary, Pankaj B. Miniyar, Y. Shyma Mary, K. S. Resmi, C. Yohannan Panicker, Stevan Armaković, Sanja J. Armaković, Renjith Thomas, and B. Sureshkumar, "Synthesis and Spectroscopic Study of Three New Oxadiazole Derivatives with Detailed Computational Evaluation of Their Reactivity and Pharmaceutical Potential," *Journal of Molecular Structure* 1173 (2018): 469–80.
37. P. R. K. Rani, Y. S. Mary, A. Fernandez, S. A. Priya, Y. S. Mary, and R. Thomas, "Single Crystal XRD, DFT Investigations and Molecular Docking Study of 2-((1,5-Dimethyl-3-Oxo-2-Phenyl-2,3-Dihydro-1H-Pyrazol-4-yl)Amino)Naphthalene-1,4-Dione as a Potential anti-Cancer Lead Molecule," *Computational Biology and Chemistry* 78 (2019): 153–64.
38. Y. Sheena Mary, Y. Shyma Mary, Renjith Thomas, B. Narayana, S. Samshuddin, B. K. Sarojini, Stevan Armaković, Sanja J. Armaković, and Girinath G. Pillai, "Theoretical Studies on the Structure and Various Physico-Chemical and Biological Properties of a Terphenyl Derivative with Immense anti-Protozoan Activity," *Polycyclic Aromatic Compounds* (2019): 1. <https://doi.org/10.1080/10406638.2019.1624974>